Elastic wavefield modelling in 3D by fourth-order staggered-grid finite difference technique

Zhengsheng Yao and Gary F. Margrave

ABSTRACT

The velocity-stress finite-difference formulation for wave propagation through 3D elastic media is presented. The wave equations are solved by a finite-difference scheme using fourth-order spatial operators and a second order temporal operator on a staggered grid. The condition for the stability and dispersions are discussed.

INTRODUCTION

Modern computational power makes possible realistic simulations of elastic wavefields at frequencies of interest. The most general numerical methods for modelling are grid-based techniques that track the wavefield on a dense 3D grid of points, e.g. the finite-difference, finite-element and pseudospectral methods. The study of wavefield propagation with 3D finite-difference methods has contributed to a better understanding of wave-path effects and the response of complex structures. The approach using a staggered grid in finite-difference methods has the advantage of accuracy with less computational effort because it allows a larger grid size.

The staggered-grid finite-difference algorithm solves the first-order elastodynamic equations of motion expressed in terms of velocity and stress. In seismic applications, the velocity-stress formulation was first used by Madariaga (1976) to model fault-rupture dynamics. This technique was extended to model seismic wave propagation in 2D media (Virieux, 1984, 1986; Levander, 1988) and 3D media (Randall, 1989). The advantages this formulation are (1) source insertion can be expressed by velocity or stress; (2) a stable and accurate representation for a planar free-surface boundary is easily implemented; (3) since the finite-difference operator are local, the entire model does not have to reside in memory at once; (4) it is easily extended to high-order spatial difference operators and (5) the algorithm is easily implemented on scalar, vector, or parallel computers.

EQUATIONS OF MOTION

Based on elastic wave theory, the equations describing elastic wave propagation within 3D, linear, isotropic elastic media can be written as

$$\begin{aligned}
\rho \partial_{tt} u_x &= \partial_x \tau_{xx} + \partial_y \tau_{xy} + \partial_z \tau_{xz} + f_x \\
\rho \partial_{tt} u_y &= \partial_x \tau_{xy} + \partial_y \tau_{yy} + \partial_z \tau_{yz} + f_y \\
\rho \partial_{tt} u_z &= \partial_x \tau_{xz} + \partial_y \tau_{yz} + \partial_z \tau_{zz} + f_z
\end{aligned} \tag{1}$$

and the stress-strain relations describe the material behaviour as

$$\begin{aligned}
\tau_{xx} &= (\lambda+2\mu)\partial_x u_x + \lambda(\partial_y u_y + \partial_z u_z) \\
\tau_{yy} &= (\lambda+2\mu)\partial_y u_y + \lambda(\partial_x u_x + \partial_z u_z) \\
\tau_{zz} &= (\lambda+2\mu)\partial_z u_z + \lambda(\partial_x u_x + \partial_y u_y) \\
\tau_{xy} &= \mu(\partial_y u_x + \partial_x u_y) \\
\tau_{xz} &= \mu(\partial_z u_x + \partial_x u_z) \\
\tau_{yz} &= \mu(\partial_z u_y + \partial_y u_z)
\end{aligned} \tag{2}$$

In the equations above, (u_x,u_y,u_z) are the displacement components; $(\tau_{xx}, \tau_{yy}, \tau_{zz}, \tau_{xy}, \tau_{xz}, \tau_{yz})$ are the stress components; (f_x, f_y, f_z) are the body-force components; ρ is the density; λ and μ are Lame constants and the symbol ∂_α is the shorthand representations of $\partial/\partial\alpha$.

The equations in (1) can be formulated into a set of first-order differential equations by first differentiating equations (2) with respect to time and then substituting the velocity components (v_x, v_y, v_z) for the time-differentiated displacements. The resulting sets of equations can be written as

$$\begin{aligned}
\partial_t v_x &= \frac{1}{\rho}(\partial_x \tau_{xx} + \partial_y \tau_{xy} + \partial_z \tau_{xz} + f_x) \\
\partial_t v_y &= \frac{1}{\rho}(\partial_x \tau_{xy} + \partial_y \tau_{yy} + \partial_z \tau_{yz} + f_y) \\
\partial_t v_z &= \frac{1}{\rho}(\partial_x \tau_{xz} + \partial_y \tau_{yz} + \partial_z \tau_{zz} + f_z)
\end{aligned} \tag{3}$$

and

$$\begin{aligned}
\partial_t \tau_{xx} &= (\lambda+2\mu)\partial_x v_x + \lambda(\partial_y v_y + \partial_z v_z) \\
\partial_t \tau_{yy} &= (\lambda+2\mu)\partial_y v_y + \lambda(\partial_x v_x + \partial_z v_z) \\
\partial_t \tau_{zz} &= (\lambda+2\mu)\partial_z v_z + \lambda(\partial_x v_x + \partial_y v_y) \\
\partial_t \tau_{xy} &= \mu(\partial_y v_x + \partial_x v_y) \\
\partial_t \tau_{xz} &= \mu(\partial_z v_x + \partial_x v_z) \\
\partial_t \tau_{yz} &= \mu(\partial_z v_y + \partial_y v_z)
\end{aligned} \tag{4}$$

Equations (3-4) can be easily solved by finite differences because the equations are all first-order in their derivatives.

FINITE-DIFFERENCE IMPLEMENTATION

The staggered grid defines some of the velocity and stress components shifted from the locations of other components by half the grid length in space (Figure 1). One of the attractive features of the staggered-grid approach is that the various difference operators are all naturally centred at the same point in space and time. The system is not only staggered on a spatial grid but also temporally, which means that the velocity field can be updated independently from the stress field. This makes the scheme efficient and concise.

By using second-order approximation for time derivatives, the solution of equations (3-4) can be expressed in a discrete form by

$$\begin{aligned}
v_{x|i,j,k}^{n+1/2} &= v_{x|i,j,k}^{n-1/2} + \Delta t b_x (D_x \tau_{xx} + D_y \tau_{xy} + D_z \tau_{xz})\,|_{i,j,k}^{n} \\
v_{y|i+1/2,j+1/2,k}^{n+1/2} &= v_{y|i+1/2,j+1/2,k}^{n-1/2} + \Delta t b_y (D_x \tau_{xy} + D_y \tau_{yy} + D_z \tau_{yz})\,|_{i+1/2,j+1/2,k}^{n} \\
v_{z|i+1/2,j,k+1/2}^{n+1/2} &= v_{x|i+1/2,j,k+1/2}^{n-1/2} + \Delta t b_z (D_x \tau_{xz} + D_y \tau_{yz} + D_z \tau_{zz})\,|_{i+1/2,j,k+1/2}^{n}
\end{aligned} \tag{5}$$

and

$$\begin{aligned}
\tau_{xx|i+1/2,j,k}^{n+1} &= \tau_{xx|i+1/2,j,k}^{n+1} + \Delta t[(\lambda+2\mu) D_x v_x + \lambda (D_y v_y + D_z v_z)]\,|_{i+1/2,j.k}^{n+1/2} \\
\tau_{yy|i+1/2,j,k}^{n+1} &= \tau_{yy|i+1/2,j,k}^{n+1} + \Delta t[(\lambda+2\mu) D_y v_y + \lambda (D_x v_x + D_z v_z)]\,|_{i+1/2,j.k}^{n+1/2} \\
\tau_{zz|i+1/2,j,k}^{n+1} &= \tau_{zz|i+1/2,j,k}^{n+1} + \Delta t[(\lambda+2\mu) D_z v_z + \lambda (D_x v_x + D_y v_y)]\,|_{i+1/2,j.k}^{n+1/2} \\
\tau_{xy|i,j+1/2,k}^{n+1} &= \tau_{xy|i,j+1/2,k}^{n+1} + \Delta t[\mu_{xy} (D_y v_x + D_y v_y)]\,|_{i,j+1/2,k}^{n+1/2} \\
\tau_{xz|i,j,k+1/2}^{n+1} &= \tau_{xz|i,j,k1/2}^{n+1} + \Delta t[\mu_{xz} (D_z v_x + D_x v_y)]\,|_{i,j,k+1/2}^{n+1/2} \\
\tau_{yz|i+1/2,j+1/2,k+1/2}^{n+1} &= \tau_{yz|i+1/2,j+1/2,k+1/2}^{n+1} + \Delta t[\mu_{xyz} (D_z v_y + D_y v_z)]\,|_{i+1/2,j+1/2.k+1/2}^{n+1/2}
\end{aligned} \tag{6}$$

In the equations above, the superscripts refer to the time index, and the subscripts refer to the spatial index. Δt is the time step and D_α represents the central finite difference operator of the spatial derivatives of ∂_α with respected to variable α. The effective parameters for the buoyancy (defined as $1/\rho$) and the rigidity μ are given by (Graves, 1996)

$$\begin{aligned}
b_x &= (b_{i,j,k} + b_{i+1,j,k})/2 \\
b_y &= (b_{i,j,k} + b_{i,j+1,k})/2 \\
b_z &= (b_{i,j,k} + b_{i,j,k+1})/2
\end{aligned} \tag{7}$$

and

$$\begin{aligned}\mu_{xy} &= (1/\mu_{i,j,k} + 1/\mu_{i+1,j,k} + 1/\mu_{i,j+1,k} 1/\mu_{i+1,j+1,k})/4 \\ \mu_{xz} &= (1/\mu_{i,j,k} + 1/\mu_{i+1,j,k} + 1/\mu_{i,j,k+1} + 1/\mu_{i+1,j,k+1})/4 \\ \mu_{yz} &= (1/\mu_{i,j,k} + 1/\mu_{i,j+1,k} + 1/\mu_{i,j,k+1} + 1/\mu_{i,j+1,k+1})/4\end{aligned} \tag{8}$$

The effective parameters can provide a more accurate representation of the actual parameters in the region near media interfaces by appropriately satisfying the traction continuity condition across the interface (Zahradnik et al., 1993).

The differential operators only act on the wavefield variables, differencing of the media coefficients is not necessary in this scheme, and the complexity of the media has no impact on the form of the differential terms. Therefore, the scheme can handle arbitrary media. The time updated wavefields are computed such that the velocity field at time $n+\Delta t/2$ is determined explicitly by using the velocity field at time $n-\Delta t$ and the stress field at time $n\Delta t$. Therefore, the time update scheme is very straightforward, and source implementation (stress, velocity and so on) is explicit and can be accomplished by simply adding the source component to the wavefield.

FOURTH ORDER DIFFERENTIAL OPERATOR

In the equations above, the spatial derivatives are given by the form of

$$\frac{\partial}{\partial \alpha} v_\alpha \approx D_\alpha v_{\alpha|i,j,k} \tag{9}$$

where D_x represents the discrete form of the differential operator $\partial/\partial x$ acting on the variable v_x, and evaluated at the point $x=i\Delta x$, $y=j\Delta y$ and $z=k\Delta z$. With a uniform grid spacing of h, the fourth-order differential operator can be written as (Levander, 1988)

$$D_x v_{x|i,j,k} = [\frac{9}{8}(v_{x|i+1/2,j,k} - v_{x|i-1/2,j,k}) - \frac{1}{24}(v_{x|i+3/2,j,k} - v_{x|i-3/2,j,k})]/h \tag{10}$$

The differential operator can also be expressed as

$$D_x v_{x|i,j,k} = [\frac{9}{8}(v_{x|i-1/2,j,k} - v_{x|i+1/2,j,k}) - \frac{1}{24}(v_{x|i-3/2,j,k} - v_{x|i+3/2,j,k})]/h \tag{11}$$

If we name (10) as the forward difference in x direction, (11) is the backward difference in x direction. Alternate use of forward and backward differential operators can maintain greater accuracy than of using only one of them.

STABILITY CONDITION ANALYSIS

The stability condition will be only analyzed under the case of a homogeneous medium. Assume that the errors of velocity and stress components (at time $m\Delta t$ and $x=ih$, $y=jh$ and $z=kh$) have the harmonic form, i.e. velocity components (for example) are

$$\begin{bmatrix} e(u_x) \\ e(u_y) \\ e(u_z) \end{bmatrix} = \begin{bmatrix} A \\ B \\ C \end{bmatrix} \exp[i(-\omega m\Delta t + k_x ih + k_y jh + k_z kh)] \tag{12}$$

where ω is an angular frequency, k_x, k_y and k_z are the components of the wavenumber k. Substituting (12) into equation (5) can lead to the equations system as (Moczo et al., 2000),

$$\begin{bmatrix} A \\ B \\ C \end{bmatrix} \left(\frac{h\sin(\omega\Delta t/2)}{\Delta t}\right)^2 = \begin{bmatrix} (\alpha\xi)^2 + \beta^2\Sigma & \alpha^2\xi\varsigma & \alpha^2\xi\eta \\ \alpha^2\xi\varsigma & (\alpha\varsigma)^2 + \beta^2\Sigma & \alpha^2\varsigma\eta \\ \alpha^2\xi\eta & \alpha^2\varsigma\eta & (\alpha\eta)^2 + \beta^2\Sigma \end{bmatrix} \tag{13}$$

where, α and β are P-wave and S-wave velocity, respectively, and

$$\xi = a\sin(3hk_x/2) + b\sin(2hk_x/2)$$
$$\varsigma = a\sin(3hk_y/2) + b\sin(2hk_y/2)$$
$$\eta = a\sin(3hk_z/2) + b\sin(2hk_z/2)$$

where, a=9/8 and b=1/24, and

$$\Sigma = \xi^2 + \varsigma^2 + \eta^2$$

By solving equation (13), we can obtain

$$\sin(\omega\Delta t/2) = \frac{\Delta t}{h}\alpha\Sigma^{1/2} \tag{14}$$

and

$$\sin(\omega\Delta t/2) = \frac{\Delta t}{h}\beta\Sigma^{1/2} \tag{15}$$

From equation (14), we have $\Delta t \le h\Sigma^{-1/2}/\alpha$. If we let Σ takes its maximum value of $3(a+b)^2$, then the stability condition for P-wave should be

$$\Delta t \le \frac{6h}{7\sqrt{3}\alpha} \tag{16}$$

and similarly, the stability condition for S-wave should be

$$\Delta t \le \frac{6h}{7\sqrt{3}\beta} \tag{17}$$

Since both types of waves are generated and propagate in a media, equation (16) should be used as the stability condition.

GRID DISPERSION CONDITION

The maximum frequency that can be accurate by modelled is related to the minimum of all frequency f calculated for each unit cell. A good rule is that the wavelength should be larger than 5 times the grid size (Levander, 1988), so that

$$f < v_{\min} / 5h \tag{18}$$

where v_{min} is minimum wave velocity.

FREE SURFACE BOUNDARY

To represent a planar free-surface boundary in the staggered-grid finite-difference scheme, an accurate and numerically stable formulation can be implemented by explicitly satisfying the zero-stress condition at the free surface (e.g., Levander, 1988), i.e.

$$\tau_{zz}\,|_{z=0} = \tau_{xz}\,|_{z=0} = \tau_{yz}\,|_{z=0} = 0 \tag{19}$$

In order to implement the equation (19) for the discrete model, values of stress and velocity components need to be specified at and above the free surface boundary anti-symmetrically (e.g. Yao & Margrave, 1999). If the index for the free boundary in the z direction k, the particular values should be set as

$$\begin{aligned}
&\tau_{zz|iz=k} = 0 && \tau_{zz|iz=k-1} = -\tau_{zz|iz=k+1} \\
&\tau_{xz|iz=k-1/2} = -\tau_{xz|iz=k+1/2} && \tau_{zz|iz=k-3/2} = -\tau_{zz|iz=k+3/2} \\
&\tau_{yz|iz=k-1/2} = -\tau_{yz|iz=k+1/2} && \tau_{yz|iz=k-3/2} = -\tau_{yz|iz=k+3/2}
\end{aligned} \tag{20}$$

Using equations (20) along with equations (2), the finite difference equations for the velocity component at the free surface are

$$\begin{aligned}
D_z v_z &= -\frac{\lambda}{\lambda + 2\mu}(D_x v_z + D_y v_y)\,|_{iz=k} \\
D_z v_x &= -(D_z v_x + D_x v_z)\,|_{iz=k+1/2} - D_x v_z\,|_{iz=k-1/2} \\
D_z v_y &= -(D_z v_y + D_y v_z)\,|_{iz=k+1/2} - D_y v_z\,|_{iz=k-1/2}
\end{aligned} \tag{21}$$

Equation (21) can be solved with second-order differential operators to obtain the velocity components in the grid row just above the free surface, given the values of v at and below the free surface.

ABSORBING BOUNDARY CONDITION

There are a number of ways to apply absorbing boundary conditions. Radiation conditions may be satisfied explicitly (Clayton and Engquist, 1977; Stacey, 1988), or the solution may be tapered over a thin strip along the boundary (Cerjan et al., 1985; Loewenthal et al., 1991). To meet radiation conditions, only two fictitious strips of

nodes along the boundary for fourth order operators are required, whereas tapering generally requires more strips. Tapering is the easiest to implement, is efficient, and is used in our late simulations.

SOURCE FUNCTIONS

Three functions are commonly used as source functions and may be expressed as follows:

Gaussian function

$$g(t) = exp(-\alpha t^2) \tag{22a}$$

the first derivative of Gaussian function

$$g(t) = -2\alpha t\, exp(-\alpha t^2) \tag{22b}$$

and the second derivative of Gaussian function (the Ricker wavelet),

$$g(t) = (4\alpha^2 t^2 - 2\alpha)\, exp(-\alpha t^2) \tag{22c}$$

This last function can be written as the function of the dominant frequency is f_d, i.e.

$$g(t) = (1 - 2\pi^2 f_d^2 t^2 \exp(-\pi f_d t^2) \tag{22d}$$

SOURCE TYPES

Source waveforms such as explosive, shear, horizontal or vertical point sources may be introduced by appropriately weighting the stresses or velocities at the source node or nodes (Aboudi, 1971). Assuming that the point source is located at grid point *(iz,ix)*, three types of sources may commonly be used for different purposes of modelling and may be implemented as follows:

Pressure source: this is used as to model a *P*-wave source and can be set by the source function the stresses at the source location

$$\tau_{xx}(ix,iy,iz) = g(t) \quad \tau_{zz}(ix,iy,iz) = g(t) \tag{23a}$$

,

S wave source: this can be implemented by the source function as the velocity variables as

$$v_x(ix,iy,iz)=g(t) \qquad v_y(ix,iy,iz)=g(t) \qquad v_z(ix,iy,iz)=g(t)$$
$$v_x(ix,iy,iz-1)=-g(t)\,,\ v_y(ix,iy-1,iz)=-g(t)\,,\ v_z(ix+1,iy,iz)=g(t) \qquad (23b)$$

Normal stress/velocity source: this can be implemented simply by acting the source function on τ_{zz} or w, respectively, i.e.

$$\tau_{zz}(ix,iy,iz)=g(t) \quad w_z(ix,iy,iz)=g(t) \quad , \qquad (23c)$$

NUMERICAL EXAMPLES

Two models are used for the numerical simulation. The first model is a homogenous media with velocity α=3000/s. The size of this model is 500m×500m×500m. The second model is a two layer model with velocities α=3000/s and β=1732m/s at the upper layer, α=4000/s and β=2000m/s at the lower layer. The size of this model is 1000m×1000m×1000m. The interface is located at the depth 650m. The grid size used for the finite difference is 5m×5m×5m and the time step is 0.0005s. A vertical force with a Ricker wavelet is located at the central of both models. The wavefields propagating in both models are horizontally symmetric. The result from the first model is shown in Figure 2. From the figure we can see that the wavefield is well simulated. Figure 3 shows the result from the second model. When the wave hit the interface, S-wave is generated on the both sides of the interface. Figure 3b shows also that the tapering boundary condition works well when the wave propagates to the bottom side of the model.

CONCLUSIONS

The Fourth-order finite difference scheme on staggered grids solving velocity-stress wave equations is presented for simulating elastic wavefield propagation in inhomogeneous isotropic media. Boundary conditions, source functions and source types are discussed in relation to the practical implementations. Numerical examples indicate that the scheme works and stable.

We plan to use this code to study the 3D elastic response of complex structures such as those in the Alberta Foothills.

ACKNOWLEDGEMENTS

We thank the sponsors of the CREWES Project for their financial support.

REFERENCES

Aboudi, J., 1971, Numerical simulation of seismic sources: Geophysics, **36**, 810-821.

Clayton, R. and Engquist, B., 1977, Absorbing boundary conditions for acoustic and elastic wave equations, Bull. Seis. Soc. Am., **67**, 1529-1540.

Graves, R.W., 1996, Simulating seismic wave propagation in 3D elastic media: Geophysics **86**, 1091-1106.

Levander, A.R., 1988, Fourth-order finite-difference P-SV seismograms: Geophysics **53**, 1425-1436.

Loewenthal, D., Wang, C.J., Johnson, O.G. and Juhlin, C., 1991, High order finite difference modeling and reverse time migration: Exploration Geophysics, **22**, 533-545.

Madariaga, R., 1976, Dynamics of an expanding circular fault: Bull. Seism. Soc. Am. **66**, 163-182.

Randall, C.J., Scheibner, D.J. and Wu, P.T., 1991, Multiple borehole acoustic waveforms. Geophysics **56**, 1757-1769.

Virieux,J., 1984, SH wave propagation in heterogeneous media: velocity-stress finite-difference method. Geophysics, **51**, 889-901.

White, J.E., 1982, Computed waveforms in transversely isotropic media. Geophysics, **44**, 771-783.

Zahradnik, J., Moczo, P. and Horn, H., 1993, Testing four elastic finite-difference schemes for behavior at discontinuities. Bull. Seism. Soc. Am. **83**, 107-129.

Yao Z. and Margrave, G.F., 1999. Fourth-order finite-difference scheme for P and SV wave propagation in 2D transversely isotropic media. CREWES Research Report, Vol. **11**

FIGURES

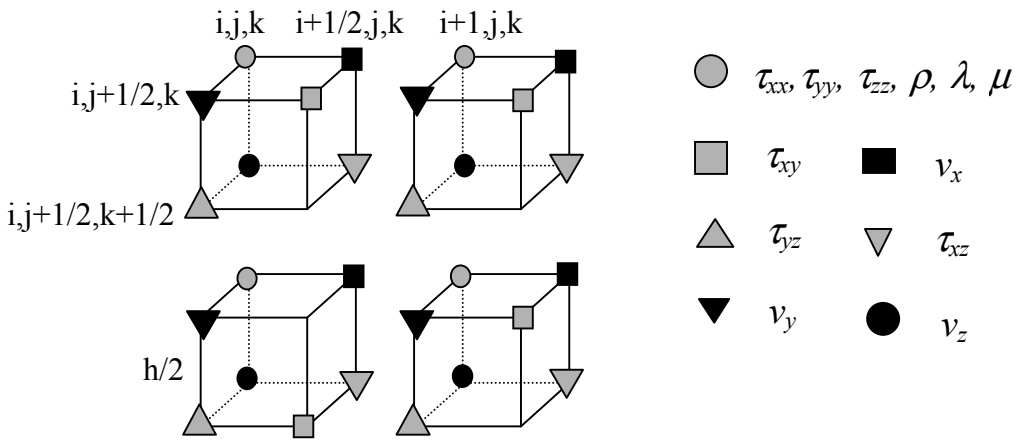

Fig. 1. A unit cell for staggered formulation consists of the wavefield variables and media parameters that are defined at a specific node. The model space is then made up of series of repeated unit cells that occupy a 3D volume of space. The indices *(i, j, k)* represent values of the spatial coordinates *(x, y, z)*, respectively, and the grid spacing *h* is defined as the length between the centres of two adjacent grid cells.

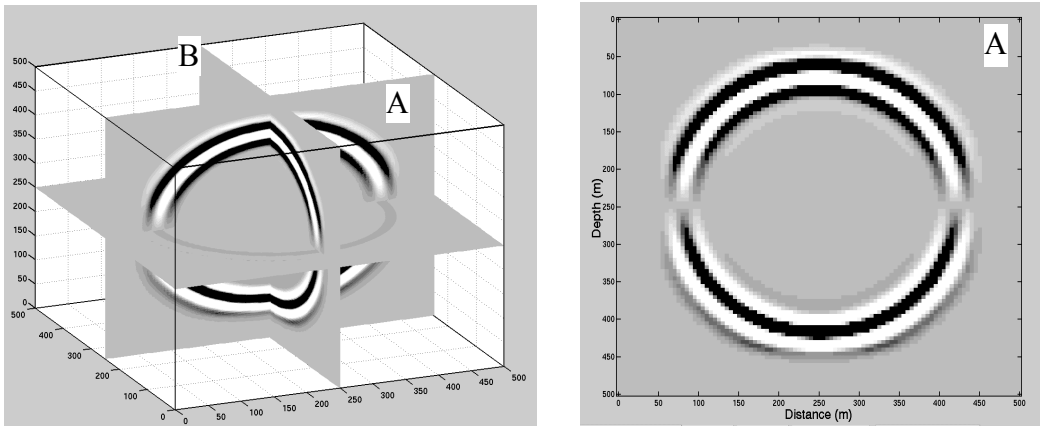

Fig. 2. The result of the simulation from the first model. Left: the two cross-sections. Right: section A from left.

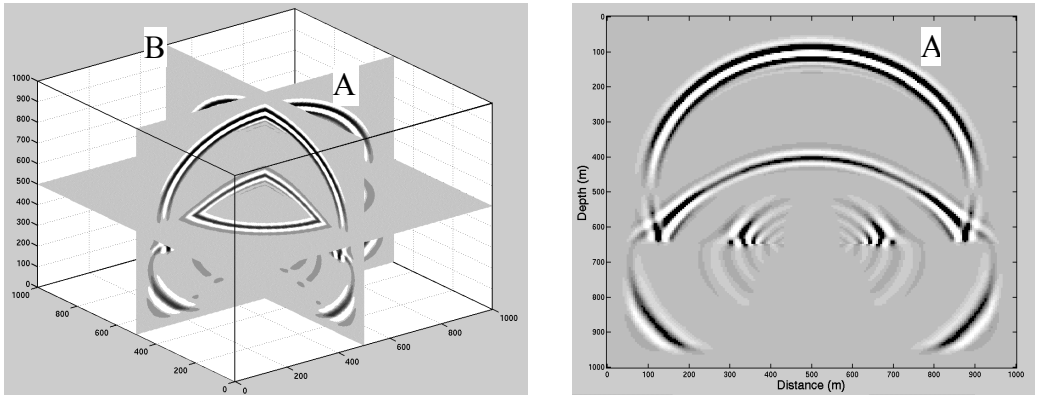

Fig. 3. The result of the simulation from the second model. Left: the two cross-sections. Right: section A from left.